Unsteady CFD of a Marine Current Turbine using OpenFOAM with Generalised Grid Interface

Thomas P. Lloyd[†*], Stephen R. Turnock[†] and Victor F. Humphrey[‡]

[†]Fluid-Structure Interactions Research Group; [‡]Institute of Sound and Vibration Research, University of Southampton, Southampton, UK. SO17 1BJ

1   Introduction

Marine current turbines (MCTs), such as the 'Seaflow' and 'Seagen' devices (Fraenkel, 2007) represent an important technology for harnessing marine renewable energy. The hydrodynamic behaviour of such devices includes complex interactions between the turbine and ocean turbulence, as well as turbine wakes if sited in arrays. These should be accounted for in performance assessments.

Traditionally, blade element momentum (BEM) models have been used to assess turbine performance, either in isolation (Batten et al., 2007) or array configuration (Turnock et al., 2011), the later study combining this approach with computational flud dynamics (CFD) simulations to model turbine wakes. Recently however, modelling the unsteady performance of turbines using viscous CFD has become more popular for the assessment of transient performance and blade fatigue loads (Faudot and Dahlhaug, 2011; Lawson et al., 2011) which are important for determining operational lifecycles. This is possible through the use of unsteady CFD techniques such as unsteady Reynolds-averaged Navier Stokes (URANS) solvers and dynamic meshing.

This paper presents the initial findings of a study carried out using the CFD library OpenFOAM® to predict the performance of a single turbine in a test tunnel environment, with comparison to the experiments of Bahaj et al. (2007). The main aim is to establish the use of dynamic meshing for conducting unsteady CFD simulations of turbomachines, with possible other applications including ship hull-propeller-rudder interaction.

2   The OpenFOAM Generalised Grid Interface

OpenFOAM is an open source CFD 'library' written using the object-oriented language C++ to solve computational continuum mechanics (CCM) problems (Weller et al., 1998). The advantage of this approach is that the user can easily interact with the top-level code and existing applications to solve CCM problems, or modify the code to create new solvers and utilities for specific user requirements. Users are also free to share their code developments with the OpenFOAM community. This has led to various 'development' releases of the code, such as that distributed under the OpenFOAM®-Extend Project.

A notable development of the code, utilised here, is the Generalised Grid Interface (GGI) (Beaudoin and Jasak, 2008), available through the Extend Project. This provides the ability to couple non-conformal mesh regions, and has been applied to numerous turbomachinery problems for handling the interface between rotating and stationary domains (e.g. see Petit et al. (2011)). The GGI passes flow variables across the interface between 'master' and 'slave' patches at each simulation time step.
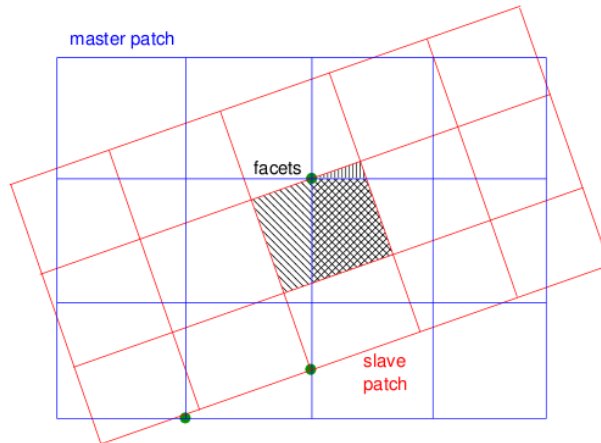

Figure 1: Schematic of master and slave patch face cutting (taken from Jasak (2011))

---

[*]*corresponding author's e-mail*: T.P.Lloyd@soton.ac.uk

This is achieved by:

1. cutting faces on the interface into facets, as shown in Figure 1;

2. calculating interpolation weights between master and slave patches based on facet areas;

3. transferring flow variables between master and slave patches using calculated weights.

Constraints for consistency and conservativeness are also invoked.

3 Case Setup

The simulated case uses the rotor geometry and experimental performance data of Bahaj et al. (2007), who tested a model-scale turbine in the QinetiQ cavitation tunnel at Haslar, Gosport, for a number of tip speed ratios (TSRs) and hub pitch angles. The main parameters of the experiments are provided in Table 1. Figure 2 shows the turbine as tested in the cavitation tunnel. The speed value quoted in Table 1 corresponds to a single tested case, with the hub pitch angle set accordingly to match the setup of Bahaj et al. (2007).

Table 1: Cavitation tunnel and turbine particulars

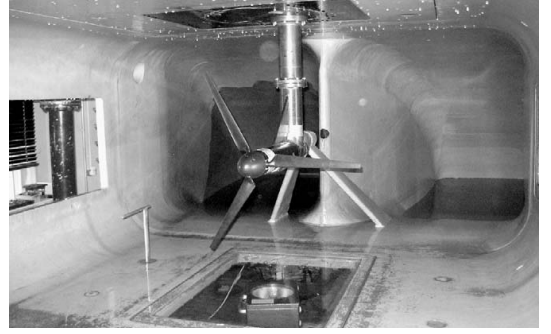| Tunnel	
Length	5 m
Breadth	2.4 m
Height	1.2 m
Maximum speed	8 ms^{-1}
Pressure	0.2-1.2 atm.
Turbine	
Rotor radius (R)	0.4 m
Hub pitch angle	25 deg
Blade shape	NACA 63-8xx
Speed (U_∞)	1.54 ms^{-1}
Tip speed ratio	6

Figure 2: Model-scale turbine in cavitation tunnel (taken from Bahaj et al. (2007))

The simulation is set up using two mesh domains created using the 'blockMesh' utility, as show in Figure 3a, to replicate the dimensions given in Table 1. Mesh refinement around the turbine blades and hub is achieved using 'snappyHexMesh'. An additional refinement is included in the form of a cylinder extending downstream from the blade tips, in an attempt to capture the tip vortices (see Figure 3b). The mesh in the far field remains unrefined, meaning the tunnel wall boundary layers are not fully resolved. The implications of this are discussed in Section 4. The simplified geometry, created using *.stl* files, is also shown in Figure 3b, assuming the hub radius to be at 20% of the radius. The boundary conditions for velocity are summarised in Table 2, referring to Figure 3. Note that the GGI upstream of the rotor is located at $x/D = -0.625$, whilst the rotating domain has a diameter of 1 metre.
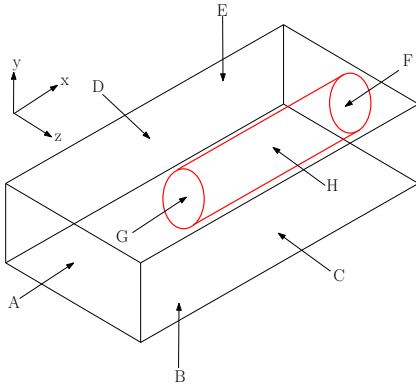
(a) Overall domain schematic
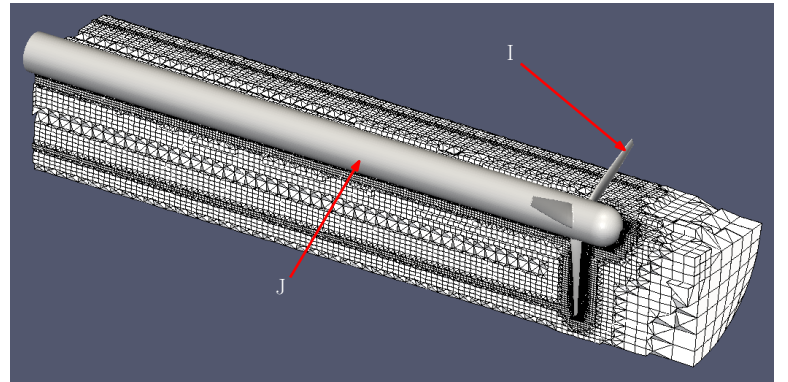
(b) Mesh cutaway view near turbine

Figure 3: Views of simulation domain with labelled patches, corresponding to Table 2

The velocity across the inlet is specified as uniform since no information is available regarding velocity profile or fluctuations from the experiments. Similarly k and ω values are assigned using the empirical formulae $k = 1.5(|u|I)^2$ and $\omega = C_\mu^{-1/4}k^{1/2}/L$, where $C_\mu = 0.09$ (Tu et al., 2008).

Table 2: Summary of boundary conditions applied to simulation domain (see Figure 3 for patch designations)

Designation	Description	BC type	Designation	Description	BC type
A	inlet	Dirichlet (fixed value)	F	outlet	Neumann
B	bottom	no slip (fixed wall)	G	GGI	ggi
C	side	no slip (fixed wall)	H	GGI	ggi
D	side	no slip (fixed wall)	I	blades	no slip (moving wall)
E	top	no slip (fixed wall)	J	hub	no slip (moving wall)

The main mesh and solver settings are presented in Table 3. The time step is controlled by imposing a limit on the maximum Courant number (Co) of 10. The resulting mean Co is approximately 0.15. This high Courant number is permitted by using the 'transientSimpleDyMFoam' solver available through the Extend Project. This allows large time steps to be used for unsteady simulations by utilising the Semi-Implicit Pressure-Linked Equations (SIMPLE) solution method.

Table 3: Mesh and simulation settings

Parameter	Setting
Mesh type	hexahedra
Mesh size	$\sim$700,000
Simulation type	URANS
Turbulence model	$k - \omega$ SST
Coupling	SIMPLE
Δt	$\sim$0.001s

4   Results and Discussion

The mesh used in this paper is considered to be extremely coarse, whilst simulations using larger meshes, $\sim$6M cells, are currently in progress. However, the results which can be extracted from the current simulation allow insight into modifications required to improve the flow feature capture and design of GGI meshes.

Figure 4 shows the time histories of turbine power coefficient and efficiency, which are defined as $C_P = P/0.5\pi\rho U_\infty^3 R^2$ and $\eta = P/\Delta P_f$ respectively, where ρ is fluid density and ΔP_f is the rate of work input from the fluid. These measures are output from the code using the 'turboPerformance' utility, available through the Extend Project.

(a) Turbine power coefficient
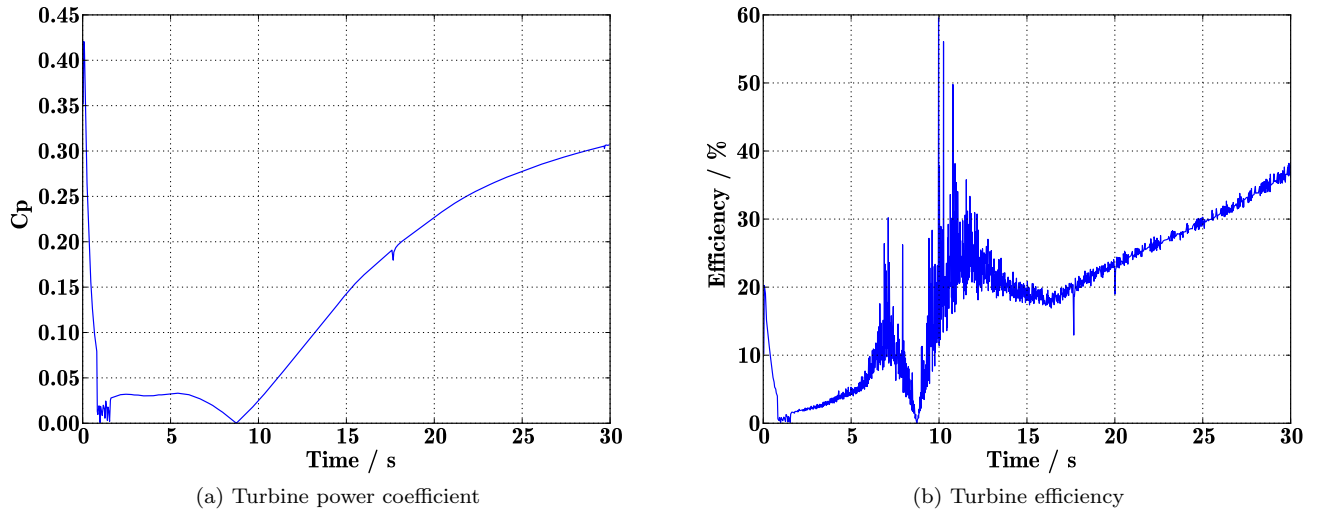
(b) Turbine efficiency

Figure 4: Non-dimensional turbine performance parameter evolution

The large fluctuations and lack of steady mean show that the solution has not fully converged. This is confirmed by examining the simulation residuals, whereby the lateral and vertical velocity components have only reduced by 10^{-3}. It is expected that this it due to the coarse mesh used outside of the turbine diameter. However, it can be seen that the C_P does appear to be tending towards a constant value, suggesting that the turbine torque is converging. Thus the almost linear increase in η may be attributed to the non-converging mass flux through the domain, suggesting a longer domain should be used.

Figure 5a shows an axial slice through the domain, with axial velocity non-dimensionalised as $u_x^* = u_x/U_\infty$. This plot shows clearly the interaction between the turbine blades and the tunnel wall boundary layer. Thus the mesh density in this region should be increased to better capture this behaviour. It also reveals a velocity jump across the GGI due to the coarse mesh used. Further refinement at the interface is required.

Figures 5b and 5c provide views of the spatial evolution of the turbine wake. Figure 5b clearly shows the velocity deficit due to the rotating blades. A wake mean velocity deficit is also evident in Figure 5c for each of

the downstream cut planes. However, there is a sharp velocity change across the GGI due to the coarse mesh, which could influence the wake development.

(a) Streamwise slice: domain centreline

(b) Transverse slice: turbine rotor

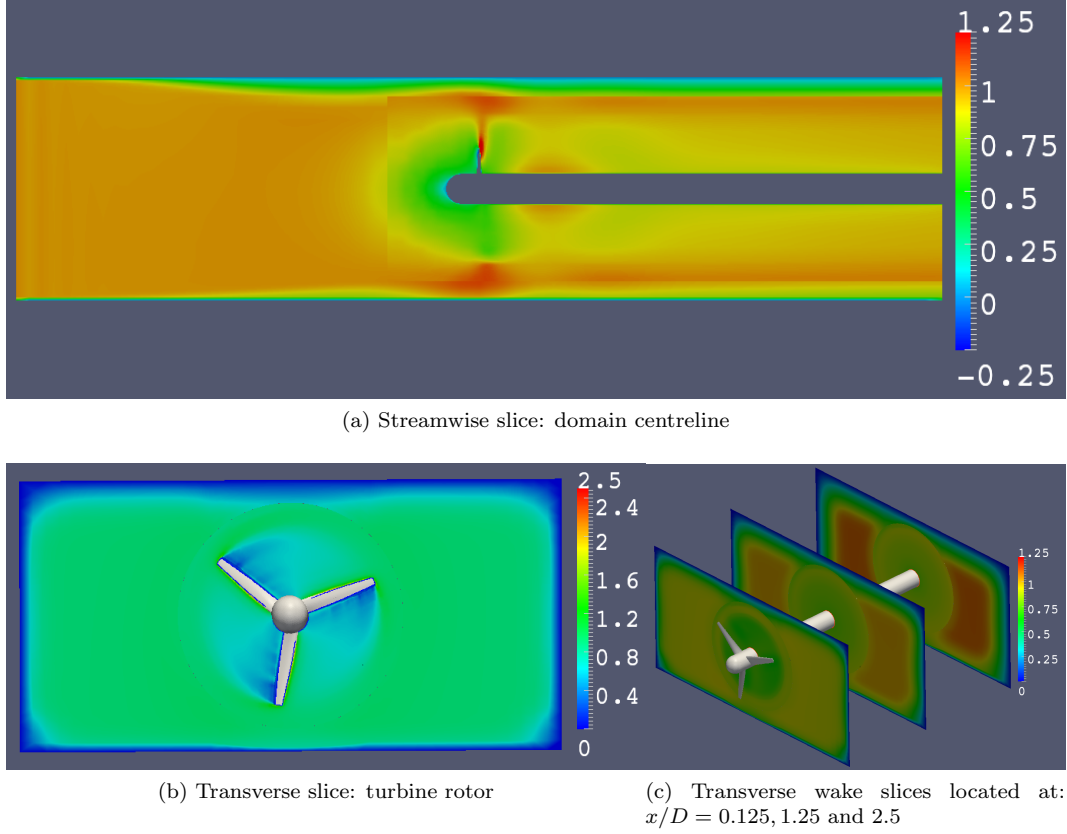(c) Transverse wake slices located at: $x/D = 0.125, 1.25$ and 2.5

Figure 5: Domain slices, displaying non-dimensional axial velocity

Of further interest is the capture of the turbulent structures in the wake, and especially the tip vortices. In order to assess this, the second invariant of the velocity tensor is used. This is calculated as $Q = 0.5(\Omega_{ij}\Omega_{ij} - S_{ij}S_{ij})$, and provides identification of vortical structures. As illustrated in Figure 6, the tip vortices of the turbine blades are captured reasonably well. However, these structures are not transported downstream a significant distance, showing the mesh to be too coarse in this region, despite some refinement being employed here (see Figure 3b). Thus furhter mesh refinement is required, which may benefit from the application of a 'vortex refinement' technique, such as that of Pemberton et al. (2002).
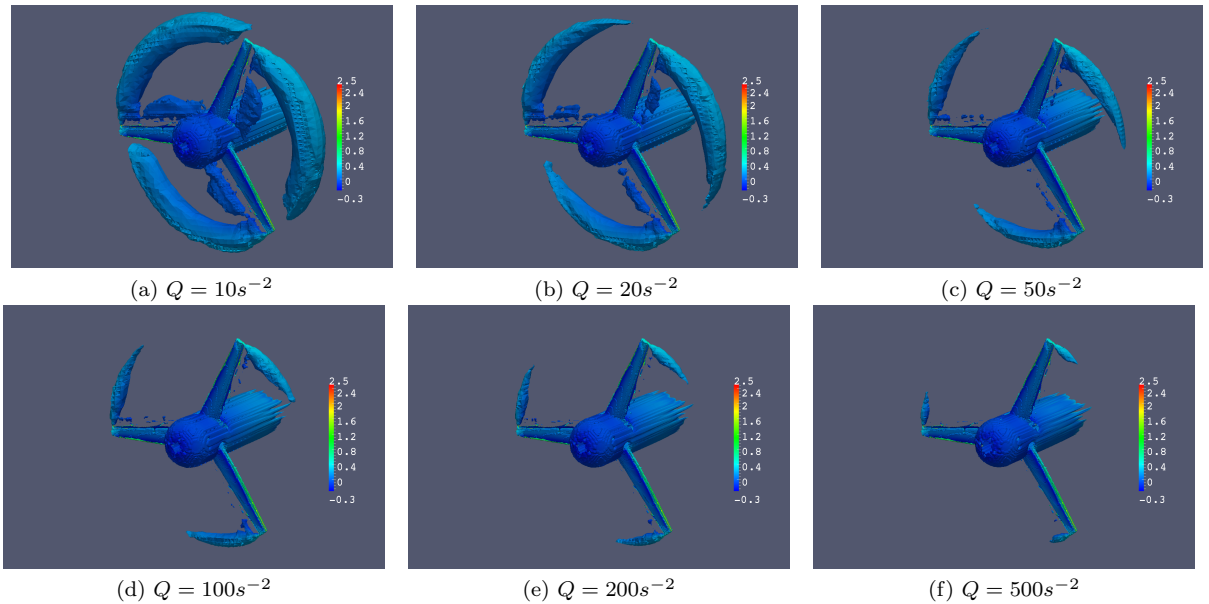

(a) $Q = 10s^{-2}$

(b) $Q = 20s^{-2}$

(c) $Q = 50s^{-2}$

(d) $Q = 100s^{-2}$

(e) $Q = 200s^{-2}$

(f) $Q = 500s^{-2}$

Figure 6: Plots of second invariant of velocity tensor, Q, coloured by non-dimensional velocity magnitude

5 Conclusions

The CFD simulation of marine current turbines under realistic conditions presents numerous challenges. The use of unsteady solution methods is important, and becoming more popular. However, accurately capturing flow features and modelling realistic conditions is not a simple task. This study has presented preliminary findings concerning the simulation of an MCT to replicate experimental performance data.

The main challenge highlighted by the results is appropriate mesh design. The coarse mesh used here has led to complex flow features and hydrodynamic interactions being lost in the simulation. The focus of future work will be on improving mesh design and using larger meshes. Furthermore, to accurately capture turbine response to realistic environmental conditions, other unsteady methods such as large- and detached-eddy simulation will be required, in order to both model ocean turbulence by specifying inlet turbulent velocities, and predict turbine response fluctuations over smaller time steps.

Acknowledgements

Nomenclature

$Co = \frac{u\Delta t}{\Delta s}$	Courant number $[-]$	$S_{ij} = \frac{1}{2}\left(\frac{\partial u_i}{\partial x_j} + \frac{\partial u_i}{\partial x_j}\right)$	Strain rate tensor $[s^{-1}]$
D	Turbine diameter $[m]$	Δs	Cell dimension $[m]$
I	Turbulence intensity $[-]$	Δt	Time step $[s]$
k	Kinetic energy $[m^2 s^{-2}]$	U_∞	Reference velocity $[ms^{-1}]$
$L = 0.07D$	Turbulence length scale $[m]$	u	Velocity $[ms^{-1}]$
P	Turbine power $[kgm^2s^{-2}]$	x	Distance downstream of rotor [m]
Q	Second invariant of velocity tensor $[s^{-2}]$	$\Omega_{ij} = \frac{1}{2}\left(\frac{\partial u_i}{\partial x_j} - \frac{\partial u_i}{\partial x_j}\right)$	Rotation rate tensor $[s^{-1}]$
R	Turbine radius $[m]$	ω	Specific dissipation $[s^{-1}]$

References

Bahaj, A., Molland, A., Chaplin, J. and Batten, W. (2007), 'Power and thrust measurements of marine current turbines under various hydrodynamic flow conditions in a cavitation tunnel and a towing tank', *Renewable Energy* **32**(3), 407–426.

Batten, W., Bahaj, A., Molland, A. and Chaplin, J. (2007), 'Experimentally validated numerical method for the hydrodynamic design of horizontal axis tidal turbines', *Ocean Engineering* **34**(7), 1013–1020.

Beaudoin, M. and Jasak, H. (2008), Development of a generalized grid interface for turbomachinery simulations with OpenFOAM, *in* 'Open Source CFD International Conference 2008', number December 2008, 4th-5th December, Berlin.

Faudot, C. and Dahlhaug, O. G. (2011), Tidal turbine blades: design and dynamic loads estimation using CFD and blade element momentum theory, *in* 'Proceedings of the 30th International Conference on Ocean, Offshore and Arctic Engineering', 19th-24th June, Rotterdam.

Fraenkel, P. L. (2007), 'Marine current turbines: pioneering the development of marine kinetic energy converters', *Proceedings of the Institution of Mechanical Engineers, Part A: Journal of Power and Energy* **221**(2), 159–169.

Jasak, H. (2011), Turbo Tools and General Grid Interface Theoretical Basis and Implementation, *in* '6th OpenFOAM workshop', number June, 13th-16th June, Penn State University.

Lawson, M. J., Li, Y. and Sale, D. C. (2011), Development and verification of a computational fluid dynamics model of a horizontal-axis tidal current turbine, *in* 'Proceedings of the 30th International Conference on Ocean, Offshore and Arctic Engineering', 19th-24th June, Rotterdam.

Pemberton, R., Turnock, S. R., Dodd, T. and Rogers, E. (2002), 'a Novel Method for Identifying Vortical Structures', *Journal of Fluids and Structures* **16**(8), 1051–1057.

Petit, O., Bosioc, A. I., Nilsson, H. k., Muntean, S. and Susan-resiga, R. F. (2011), 'Unsteady simulations of the flow in a swirl generator , using OpenFOAM', *International Journal of Fluid Machinery and Systems* **4**(1), 199–208.

Tu, J., Yeoh, G. H. and Liu, C. (2008), *Computational Fluid Dynamics: A Practical Approach*, Elsevier Ltd, Oxford.

Turnock, S. R., Phillips, A. B., Banks, J. and Nicholls-Lee, R. (2011), 'Modelling tidal current turbine wakes using a coupled RANS-BEMT approach as a tool for analysing power capture of arrays of turbines', *Ocean Engineering* **38**(11-12), 1300–1307.

Weller, H. G., Tabor, G. R., Jasak, H. and Fureby, C. (1998), 'A tensorial approach to computational continuum mechanics using object-oriented techniques', *Computers in Physics* **12**(6), 620–631.